Airway Deposition of Nebulized Gene Delivery Nanocomplexes Monitored by Radioimaging Agents

Maria D. I. Manunta[1], Robin J. McAnulty[3], Amy McDowell[4], Jing Jin[5], Deborah Ridout[2], John Fleming[6], Stephen E. Bottoms[3], Livia Tossici-Bolt[6], Geoffrey J. Laurent[3]*, Lorenzo Biassoni[4], Christopher O'Callaghan[7‡], and Stephen L. Hart[1]

[1]Wolfson Centre for Gene Therapy of Childhood Disease, and [2]Centre for Pediatric Epidemiology and Biostatistics, UCL-Institute of Child Health, University College London, London, United Kingdom; [3]Centre for Inflammation and Tissue Repair, University College London, London, United Kingdom; [4]Department of Radiology, Great Ormond Street Hospital for Children, London, United Kingdom; [5]Department of Primary Care Health Sciences, University of Oxford, Oxford, United Kingdom; [6]Department of Nuclear Medicine, Southampton University Hospitals National Health Service Trust, Southampton, United Kingdom; and [7]Department of Infection, Immunity and Inflammation, University of Leicester, Leicester Royal Infirmary, Leicester, United Kingdom

Receptor-targeted nanocomplexes are nonviral vectors developed for gene delivery to the airway epithelium for the treatment of pulmonary disease associated with cystic fibrosis. The present study aimed to optimize the delivery of the nanocomplex by nebulization, and to monitor the *in vivo* deposition of radiolabeled vector in the airways of a large animal model by γ-camera scintigraphy. Large White weaner pigs were nebulized with nanocomplexes mixed with technetium-99m radiopharmaceuticals. The aerosol deposition scans suggested that the nebulized radiovectors were deposited mainly in the trachea–main bronchi and in the midregion of the lungs. The plasmid biodistribution, assessed by real-time PCR, correlated with the scintigraphy images. The highest plasmid copy numbers were found in the bronchial areas and in the tissues proximal to the main bronchi bifurcation. Immunohistochemistry detected transgene expression in the tracheal and bronchial ciliated epithelium. Histological analysis of lung tissue showed no evidence of inflammation, and no increase in inflammatory cytokines or inflammatory cells was detected in the bronchoalveolar lavage. The deposition of nebulized nanocomplexes coassociated with technetium-99m can be monitored by nuclear medicine techniques. The use of a noninvasive strategy to follow the delivery of the vector could improve the clinical management of patients undergoing cystic fibrosis gene therapy.

Keywords: gene delivery; airways; cystic fibrosis; scintigraphy; imaging

Cystic fibrosis (CF) is an autosomal, recessively inherited disorder caused by defects in the gene encoding for the cystic fibrosis transmembrane conductance regulator (CFTR), a cyclic adenosine monophosphate–regulated chloride channel located in the apical surface of the exocrine epithelia. Pulmonary disease is the major cause of CF morbidity and mortality. The recurrent respiratory infections and inflammation result in progressive parenchymal disruption, bronchiectasis, and ultimately death from respiratory failure (1). CF remains a strong candidate for gene therapy. However, in clinical trials thus far with several different nonviral vectors (mainly comprising liposomes), gene transfer efficiencies were insufficient to anticipate any clinical benefit (2). Various strategies are undergoing investigation to improve gene delivery to the lung, including alternative delivery systems and genetic constructs for improved expression and immunogenicity. A further priority involves developing methods of administration by inhalation to ensure the maximal deposition of vector formulations to the conducting airways, the region of highest expression of endogenous CFTR and the primary target for gene therapy in CF pulmonary disease.

Aerosol delivery provides the most practical means to administer CF gene therapy vectors and radiopharmaceuticals to the respiratory tract, but the choice of nebulizer, the formulation, and the airflow rate, among other factors, can all affect the site and efficiency of delivery. Aerosol particles with an aerodynamic diameter of 1 to 5 μm can be inhaled into the airways, with smaller particles penetrating to the alveoli, and the larger particles penetrating to the trachea. Therefore, achieving the right size is critical (3). Aerosolized radioactive tracers are routinely used in the clinical setting to assess lung function and to detect early pulmonary damage or dysfunction, which are particularly useful both diagnostically and prognostically for young children with CF (4). Because these radiological techniques are already well-established clinically, they provide potentially transferrable tools to monitor gene delivery to the airways.

In this study, we investigated the deposition of nebulized receptor-targeted nanocomplex (RTN) in the airways of juvenile pigs. The RTN formulation comprises cationic liposomes, a receptor-targeting peptide and plasmid DNA that self-assembles electrostatically to form cationic nanoparticles of approximately 150 nm (5). We previously tested this vector system for the transfection of airway epithelial cells *in vitro* and *in vivo* in murine lungs and tracheas via instillation and nebulization (5–7). Pigs are used widely in preclinical studies, because their lung physiology and anatomy are closer to those of humans than are those of small rodents, and their size allows for regional studies of nebulized deposition within the lung after inhalation.

We first assessed the distribution of the nanocomplexes mixed with technetium (Tc)-99m albumin (nanocolloid) and aerosolized by the AeroEclipse II BAN Jet Nebulizer (Trudell Medical International Europe Ltd.) in the next-generation pharmaceutical impactor (NGI). This seven-stage cascade impactor allows

(*Received in original form January 22, 2013 and in final form April 9, 2013*)

* Present affiliation: Centre for Cell Therapy and Regenerative Medicine, University of Western Australia, Nedlands, Western Australia, Australia.

‡ Present affiliation: Portex Anesthesia, Department of Cardiorespiratory Sciences, UCL-Institute of Child Health, University College London, London, United Kingdom.

This work was funded by a project grant from SPARKS - for Children's Health (http://www.sparks.org.uk).

Author Contributions: M.D.I.M., R.J.M., L.B., J.F., G.J.L., C.O., and S.L.H. designed the research. M.D.I.M. and S.E.B. performed the research. L.T.-B. and D.R. contributed new reagents and analytic tools. M.D.I.M., A.M., R.J.M., and J.J. analyzed the data. M.D.I.M., L.B., A.M., C.O., and S.L.H. wrote the manuscript.

Correspondence and requests for reprints should be addressed to Stephen L. Hart, Ph.D., Wolfson Centre for Gene Therapy of Childhood Disease, UCL-Institute of Child Health, University College London, 30 Guilford Street, London WC1 N1EH, UK. E-mail: s.hart@ucl.ac.uk

This article has an online supplement, which is accessible from this issue's table of contents at www.atsjournals.org

Am J Respir Cell Mol Biol Vol 49, Iss. 3, pp 471–480, Sep 2013

Originally Published in Press as DOI: 10.1165/rcmb.2013-0030OC on April 24, 2013
Internet address: www.atsjournals.org

aerosol particle size to be estimated, thus enabling a prediction of the site of lung deposition of nebulized particles according to their terminal settling velocities, depending on their aerodynamic diameters (i.e., specific density, shape, and gravity) (8). Subsequently, we monitored the deposition of Tc-99m RTNs in pig airways by scintigraphy, and compared that deposition with the distribution of plasmid DNA according to real-time PCR. Reporter gene expression was evaluated in lung-tissue sections by immunohistochemistry to identify transfected cells. The presence or absence of inflammatory markers attributable to RTN nebulization and the cell count were assessed in the bronchoalveolar lavage (BAL) from the accessory lobe of the pig right lung, as well as in the hematoxylin and eosin staining of lung tissue sections.

MATERIALS AND METHODS

RTN Suspensions and *In Vitro* Distribution

RTNs were prepared as described elsewhere (5), whereas radiovectors were prepared by adding Tc-99m albumin (nanocolloid; Tc-99m Alb) to the nanocomplexes. The distribution of RTNs was assessed in cell culture and then *in vivo*. The suspensions of nanocomplexes were nebulized through the NGI. The RTNs deposited in the various stages of the equipment were used for cell transfections and radioactivity detection. The log-probability graphs obtained were used to determine the particle-size distribution of the aerosolized suspension (9). Further particulars are available in the online supplement.

Animals and Functional Studies

All animal procedures were approved and licensed by the United Kingdom Home Office. Eleven Large White weaner pigs were acclimatized and divided into three cohorts (Table 1). One control pig received a computed tomography (CT) scan, whereas control B1 and B2 pigs and animals of both cohorts underwent baseline scintigraphies to define the contours of their lungs, after the administration of approximately 63.5 MBq of Tc-99m albumin macroaggregates (MAAs) intravenously. After 2 days, all animals were intubated without mechanical ventilation. The control pigs were nebulized with either H_2O or Tc-99m Alb, the animals of the first cohort were treated with RTNs alone, and the second cohort was treated with RTN–Tc-99m Alb. Those receiving Tc-99m Alb underwent scintigraphy scans immediately after nebulization.

We used different methods to define the regions of interest (ROIs) and analyze the aerosol deposition in pig lungs. The assessment of airway versus parenchymal deposition was performed by calculating the central–peripheral deposition (C/P) ratio of Tc-99m activity in the aerosol scan, normalized to the activity in the perfusion scan (representing lung volume) (10). The method used was taken from Bennett and colleagues (10) and Biddiscombe and colleagues (their Method 5) (11). A second strategy was applied, defining five ROIs, including the trachea–main bronchi, apical, middle, and diaphragmatic areas of the lungs and a background/scatter. Further details are presented in the online supplement.

Gene Expression *In Vitro* and *In Vivo*

Small aliquots of RTNs and RTNs coassociated with Tc-99m Alb that were nebulized in animals were tested for their ability to transfect epithelial cell lines *in vitro*.

On Day 3 after nebulization, blood samples were taken from the pigs before culling, immediately after which the BAL was collected from the fourth lobe (accessory) of the right lung, using a clinical-grade saline solution. Whole BAL was used for cytology, whereas BAL fluid was analyzed for TNF-α and IL-6.

Pig tissues were collected from the remaining lobes of each lung (cranial, middle, and caudal, respectively). For sampling purposes, the apical lobe of the left lung was considered as two separate segments (cranial and middle). All tissue samples, with the exceptions of bronchioles and the trachea, were taken from areas proximal to the main bronchi branching. All tissues were snap-frozen in liquid nitrogen and stored at $-80^{\circ}C$ until required for plasmid DNA and RNA analysis.

Samples for histology were fixed in 4% paraformaldehyde and processed as previously described (12). Histological sections were stained for β-galactosidase or hematoxylin and eosin.

RESULTS

Comparison between Transgene Expression and Radioactivity after Nebulization of Tc-99m–Coassociated RTNs in a Next-Generation Impactor

The aerosol generated from the AeroEclipse containing the RTN formulation, mixed with Tc-99m albumin (nanocolloid), was pulled through the prechilled NGI, operated at an airflow rate of 15 L/minute. The material deposited in the different NGI stages was tested for radioactivity, using a microplate liquid scintillation counter, and was tested for plasmid DNA content through its ability to transfect the two epithelial cell lines, normal bronchial (16HBE14o−) and cystic fibrosis bronchial (CFBE41o−) (Figure 1a). The transfecting RTNs and the radioactivity counts were both found predominantly in stages 2–6 of the NGI. Although the nanocomplexes were not directly labeled with the radiopharmaceutical, the anionic albumin is likely to interact electrostatically with the cationic RTNs, and so the coassociated complexes share a similar pattern of deposition. In fact, the geometric size and the ζ potential (electrostatic charges) of the suspension containing both RTNs and Tc-99m Alb were 238 ± 2.5 nm and 42.3 ± 1.4 mV, respectively, whereas the average geometric size and the surface charge of the Tc-99m Alb (nanocolloid) alone were 150.4 ± 27.2 nm and −13.7 ± 1.1 mV, respectively.

TABLE 1. OUTLINE OF *IN VIVO* EXPERIMENTS

Groups	Animal Number	Sex	Weight (*kg*)	Injection (Intravenous)	Nebulization	Scintigraphy
Control pigs	Ctrl A	Female	39	Saline	H_2O	No scans
	Ctrl B1	Female	38	Tc-99m MAA	Tc-99m Alb	Q and AD
	Ctrl B2	Male	33	Tc-99m MAA	Tc-99m Alb	Q and AD (+ CT)
First cohort, RTNs	A1	Male	28.5	Tc-99m MAA	RTNs	Q
	A2	Male	24	Tc-99m MAA	RTNs	Q
	A3	Female	25	Tc-99m MAA	RTNs	Q
	A4	Female	29.5	Tc-99m MAA	RTNs	Q
Second cohort, radioRTNs	B1	Male	23	Tc-99m MAA	RTNs, Tc-99m Alb	Q and AD
	B2	Female	27	Tc-99m MAA	RTNs, Tc-99m Alb	Q and AD
	B3	Female	25	Tc-99m MAA	RTNs, Tc-99m Alb	Q and AD
	B4	Male	26	Tc-99m MAA	RTNs, Tc-99m Alb	Q and AD

Definition of abbreviations: AD, aerosol deposition scan; CT, computed tomography; Ctrl, control; Q, perfusion scan; RTNs, receptor-targeted nanoparticles; Tc-99m Alb, Tc-99m albumin nanocolloid; Tc-99m MAA, Tc-99m albumin macroaggregate.

The scheme of the study summarizes details of animals included in each group, their sex and weight, the radiopharmaceuticals administered, the material nebulized, and the type of scans performed.

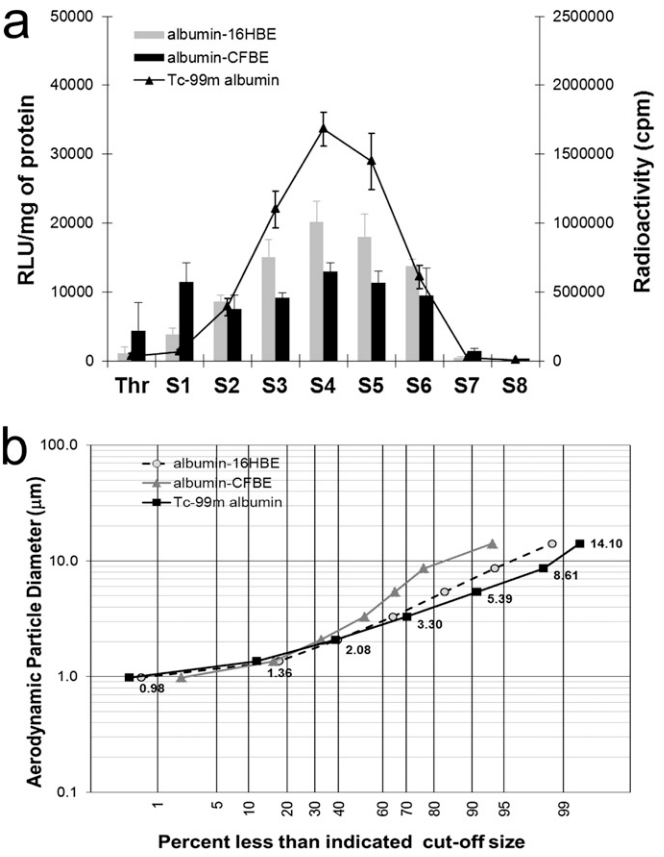

Figure 1. Comparison of transfections mediated by the radiovectors in two different cell lines and of the radioactivity in the same samples. (*a*) Transfections (*bars*) and radioactivity (*straight lines*) in normal bronchial 16HBE14o− (16HBE) and cystic fibrosis (CF) bronchial CFBE41o− (CFBE) cells are shown. Receptor-targeted nanoparticles (RTNs) (N-[1-(2,3-dioleyloxy)propyl]-N,N,N-trimethlylammoniumchloride and dioleylphosphatidylethanolamine, i.e. DOTMA/DOPE, peptide E, and pCILuc plasmid) were mixed with the radiopharmaceuticals (0.5 MBq/μg DNA) before nebulization. After aerosolization, an aliquot of nebulized material was collected and added to the scintillant fluid, and radioactivity was promptly read in a scintillation counter calibrated for technetium (Tc)–99m. Radioactivity was expressed in counts per minute (cpm). Another aliquot of the same volume was added to OptiMEM (Invitrogen) medium in the cell-culture wells. After 48 hours of incubation, luciferase expression was measured. Luciferase activity was quantified as relative light units (RLU) per mg of protein. The *error bars* represent the standard error of the mean of $n = 4$ (albumin nanocolloid) independent experiments. Thr, throat; S1–S8, stages 1–8 of the next-generation impactor (NGI). S8 involves the micro-orifice collector. (*b*) The aerodynamic size distribution of RTNs through the NGI was described in a log-normal distribution plot. Each data point is a mean of four independent experiments, determined either as radioactivity counts from the RTNs collected in the different stages, or as transfection efficiency values as a measure of the amount of DNA present in the nanocomplexes. Each data point in either plot indicates the percentage of RTNs retrieved in the NGI stages whose size cutoff was less than the indicated diameters, according to Marple and colleagues (52).

The RTNs on their own were measured at 150.0 ± 1.5 nm and 57.6 ± 0.8 mV, respectively.

In Figure 1b, the distribution of the material collected from different stages of the NGI is represented as a log-normal graph, where the *y* axis indicates the aerodynamic diameter, and the *x* axis indicates the percentage of RTNs deposited below a certain size diameter cutoff. The aerodynamic cutoff size is defined as the aerodynamic size above which a particle is aerodynamically unable to enter a stage of the impactor (9). The radioactivity associated with RTNs retrieved from the different NGI stages, or the amount of DNA from the same collection cups, measured indirectly by its ability to transfect cells *in vitro*, was used to calculate the mass median aerodynamic diameter (MMAD) and geometric standard deviation (GSD), parameters that provide indications of the central tendency of particle distribution and the spread of nanocomplexes. MMADs and GSDs were determined as described elsewhere (13). The MMADs were 2.91, 3.08, and 3.81 μm, with GSDs of 1.68, 1.81, and 2.25 μm. These values were not statistically significant according to ANOVA calculated with Stata software (Stata Statistical Software: Release 11; StataCorp, College Station, TX). Taken together, these results indicate that RTNs mixed with Tc-99m albumin could represent the distribution of the nanocomplexes themselves by aerosolization *in vivo* in a porcine model.

Imaging of Pig Lungs by Scintigraphy and Computerized Tomography

Lung perfusion scans. Lung perfusion scans were performed in pigs with Tc-99m albumin MAAs, including two control pigs and the two cohorts of four pigs each (Table 1 and Table E1 in the online supplement). The lung perfusion scan was performed to provide a visual assessment of the distribution of radiopharmaceutical in both lungs, and to assess lung function before the aerosol administration of RTNs coassociated with Tc-99m Alb. In all pigs, lung perfusion scans were assumed to represent a uniform distribution of tracer in the lungs, with a variation in intensity across the lung fields on the two-dimensional image primarily attributable to the varying thicknesses of lung tissue represented by each pixel in the image (Figure 2).

Aerosol deposition scans. The respiratory rate of resting/anesthetized pigs varied from 24–36 breaths per minute (Table E1), similar to the breathing frequency of children 1–3 years of age. The breath depth was sufficient to inhale the aerosols produced by the AeroEclipse nebulizer in breath-actuated operational mode without any further assistance, suggesting that sufficient negative pressure was generated in the nebulizer during inspiration to activate nebulization.

The lung aerosol deposition scan of the control pig receiving Tc-99m albumin nanocolloid showed a distribution of radiotracer in both lungs similar to that in the treated animals (Figure 2A). The ROIs delineating central versus peripheral lung areas (Figure 3A and Table 2) were first considered, because this is the standard way in which aerosol deposition is classically analyzed in humans (10, 11).

Chest CT scans were acquired from the control pig, and the tomogram recorded was used to detail the anatomy of the porcine lungs. Frontal, sagittal, and cross-sectional images at different levels of the body showed substantial differences from human anatomy, mainly including the cardiac notch and the accessory lobe right in the middle of the central region (Figure 3B). The bottom end of the endotracheal tube can also be clearly seen in both frontal and sagittal planes of the first CT image.

Additional ROIs considered more informative for assessing aerosol deposition in the porcine lungs were drawn (Figure 3C). The lung scans of the four pigs of the second cohort that received Tc-99m Alb RTNs showed significant deposition of the radiopharmaceutical in the distal portion of the trachea and the region proximal to the main bronchi and in the midzone of both lungs (Figures 2A, 3A, and 3C). A relative quantification of radioactivity within the ROIs around the trachea–main bronchi and the upper, mid, and lower zones of each lung, drawn in the anterior and posterior views, confirmed this finding, showing much higher counts from the trachea–bronchi and midzones in comparison with the upper (apical) zones of the lungs (Table

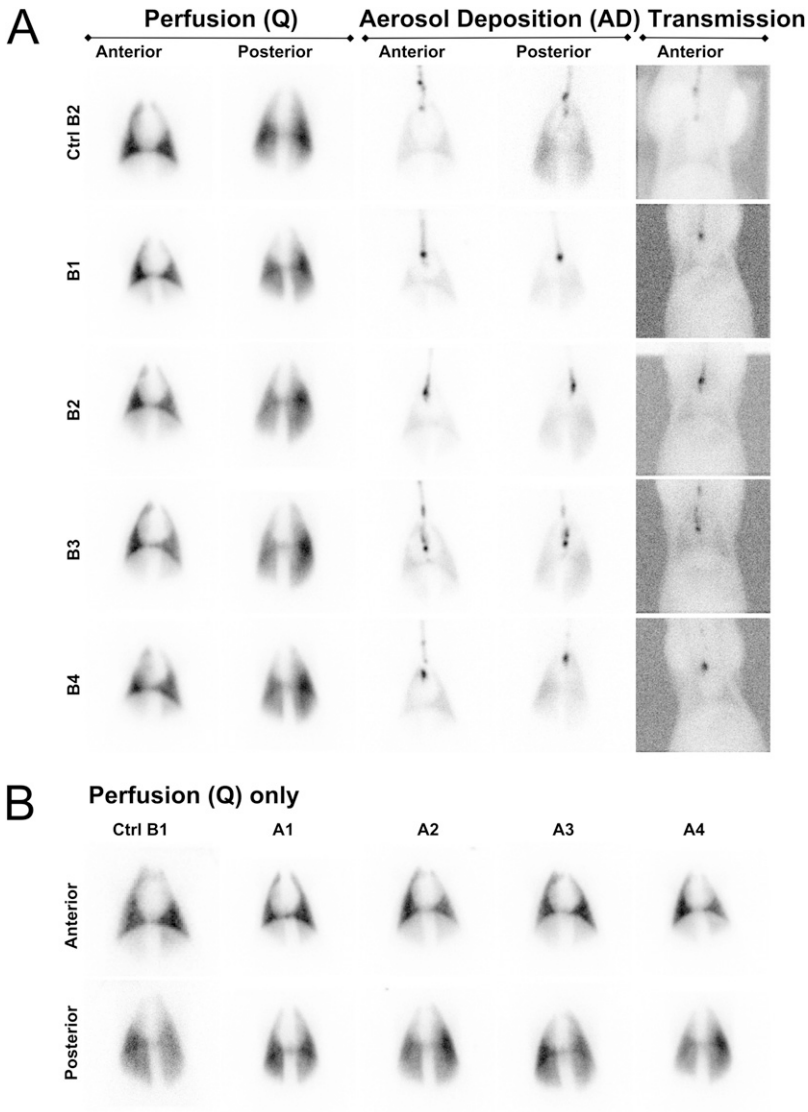

Figure 2. Perfusion, aerosol deposition, and transmission scintigraphies. (*A*) Static perfusion (Q) scans of pig lungs injected with Tc-99m macroaggregates via the ear vein of the control pig (Ctrl) and those of the second cohort (nebulized with RTNs coassociated with 99mTc-Alb) are presented side by side, with the aerosol deposition images (AD) in the same animal nebulized with either Tc-99m albumin nanocolloid or radioRTNs. Anterior (ventral) and posterior (dorsal) views are shown. In the *rightmost column,* transmission scans (ventral view) using a Co-57 rectangular flood source of the control pig and the second cohort are displayed. (*B*) Perfusion scintigraphies, as baseline of the lungs of the remaining pigs, are also represented (i.e., the control pig and the first cohort nebulized with RTNs). Images show anterior (ventral) and posterior (dorsal) views of each animal.

2). The lower (diaphragmatic) zones also showed a considerable amount of counts, probably because of the mass volume of lung tissue and the peculiar dichotomic bronchial bifurcation pattern in pigs (Figures 3B and 3C).

In Vitro Efficacy of RTNs and Radiovectors Used for *In Vivo* Nebulization

Aliquots of RTNs and Tc-99m Alb RTNs (after the decay of radioactivity) were tested for their ability to transfect airway epithelial cell lines *in vitro*. Prenebulization suspensions provided comparable transfection efficiencies in both 16HBE14o− and CFBE41o− cells (Figure 4A). Radioactive and nonradioactive RTN suspensions, remaining in the nebulizer chamber upon completion of the aerosolization *in vivo* (leftover), were also tested for their ability to deliver the reporter gene. These results confirmed that both before and after nebulization, suspensions contained efficient delivery vectors, which retained their transfecting activity at least several weeks after being used *in vivo*.

Quantitative Analysis of pCpG-Free lacZ in Airway Tissues

The biodistribution of the plasmid (copy number) was quantified by real-time PCR in airway tissue samples from different regions of the lung in each animal. In the four animals of the first cohort, which received nonradioactive RTNs, the transgene copy numbers were highest in the first bifurcation of the bronchi, in the subsegmental bronchi, and in other parts of the middle lobes, whereas fewer plasmids were detected in the caudal (diaphragmatic) and cranial (apical) lobes (Figure 4B, *top*). In the second cohort (Figure 4B, *bottom*), which comprised pigs nebulized with radiovectors, the delivered transgene was detected predominantly in the middle lobes, but also in the cranial and caudal lobes, and in the trachea of one pig. No plasmid was detected in samples analyzed from control pigs.

The samples from the same lung regions positive for plasmid copy number among pigs of the first cohort (treated with RTNs) and second cohort (aerosolized with radiovectors) were analyzed further for gene expression. Mucin 4 (Muc4) and α-tubulin acetyltransferase (α-TAT) were chosen as housekeeping genes, because both are expressed in the respiratory epithelium. Despite the low amount of transgene delivered, seven of these samples displayed increased β-galactosidase mRNA concentrations relative to α-TAT, whereas only one was positive for both Muc4 and α-TAT (Figure E1). The first three samples belonged to the RTN-treated cohort (A1, A2, and A4, respectively), and

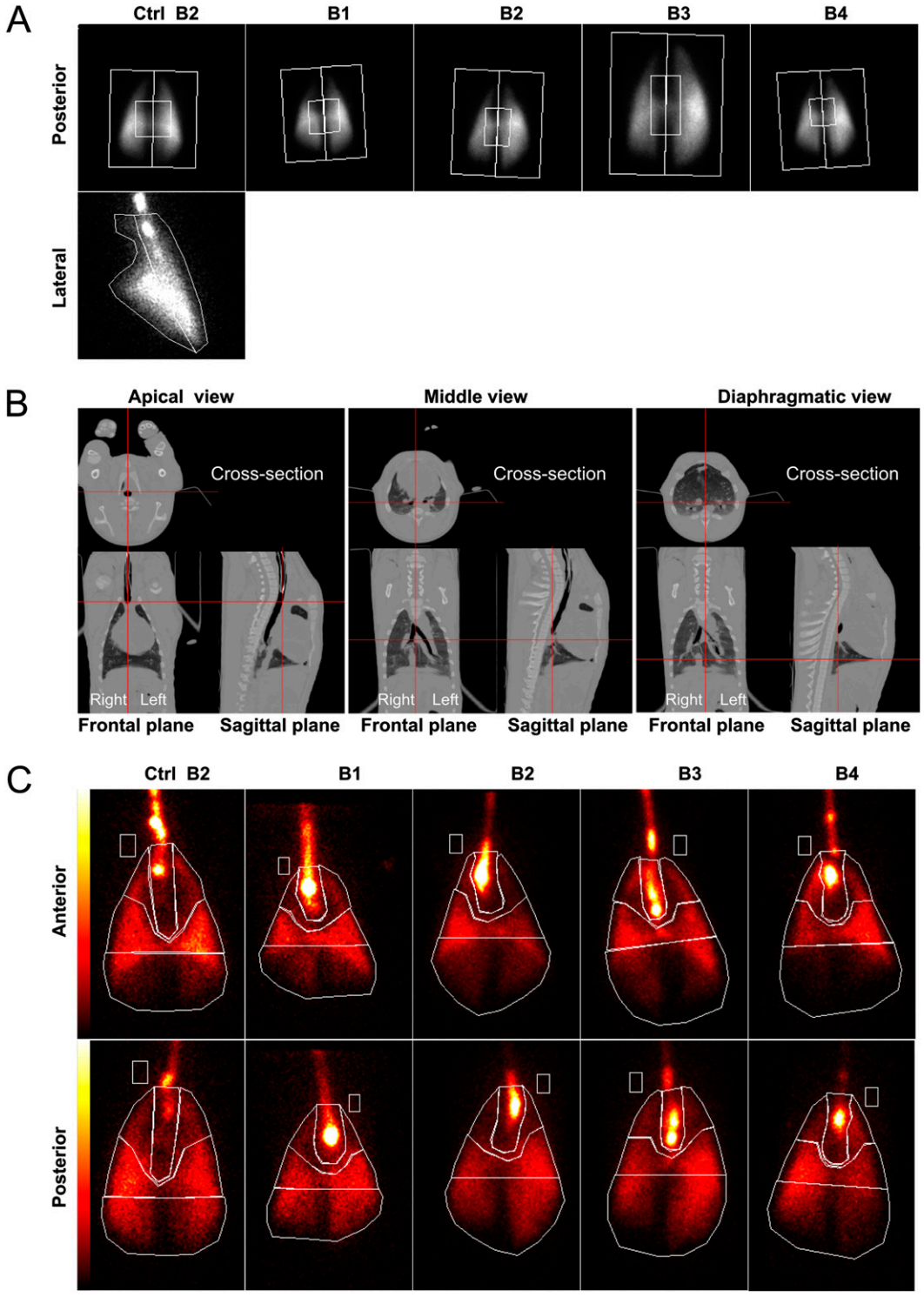

Figure 3. Aerosol deposition quantification study. (*A*) Gamma-scintigraphic posterior images of the control pig and the second cohort, aerosolized with radiovectors, were divided into central and peripheral regions of interest (ROIs). The lateral view of the control pig is also shown. (*B*) Computed tomographic images of the control pig show three different views of the frontal and sagittal planes, with positions (*red lines*) where the cross-sections were taken. (*C*) Anterior and posterior views of the ventilation of Tc-99m albumin nanocolloid in the control pig and the deposition of radioRTN aerosols. The respiratory system was divided into four different ROIs: the proximal trachea–main bronchi, the upper or apical zone, the middle area, and the diaphragmatic zone. The *rectangular region* within the pig body contour represents the scatter ROI.

the last four belonged to those nebulized with Tc-99m RTNs (B1, and two samples in B2 and B3).

Immunohistochemistry and Histology

Ciliated epithelium in the distal trachea and bronchi of two animals in the first cohort (Figure 4C, *left*) stained positively for β-galactosidase activity, with no staining in the underlying basal epithelial cells. Samples of lung tissue from the respiratory tract were also assessed for any adverse effects after the nebulization of RTNs. Histological sections showed normal mucus, healthy pseudostratified columnar ciliated epithelium, and intact subepithelial connective tissue (Figure 4C, *right*).

Analysis of Inflammation and Toxicology Testing

Previous clinical trials reported that the administration to the airways of a cationic liposome, GL67, complexed with plasmid DNA, caused febrile flu-like symptoms and inflammation in some patients (14, 15), which may have been caused by the plasmid DNA. Therefore, to reduce the potential for an immune response to the bacterial part of the plasmid DNA and to avoid

TABLE 2. RELATIVE QUANTIFICATION OF THE Tc-99m ALBUMIN NANOCOLLOID IN DIFFERENT REGIONS OF INTEREST OF PIG LUNGS

Region of interest	Ctrl B2	B1	B2	B3	B4
C/P ratio (left)	1.36	1.27	1.45	0.87	1.27
C/P ratio (right)	1.50	2.33	1.67	0.42	0.77
C/P ratio (lateral)	1.03	ND	ND	ND	ND
Diaphragmatic (%)	27	26	33	33	20
Middle (%)	43	29	28	29	38
Apical (%)	16	10	9	13	16
Trachea and main bronchi (%)	14	35	30	25	26

Definition of abbreviations: C, central; Ctrl, control; ND, not determined; P, peripheral; Tc-99m, technetium-99m.

The normalized central/peripheral count ratios were calculated considering the perfusion scan as lung volume. Relative percentages of the Tc-99m radiopharmaceutical in different areas of pig lungs were also determined. B1–B4 indicate animals belonging to the cohort treated with Tc-99m albumin nanocolloid receptor-targeted nanoparticles, whereas Ctrl B2 is a control pig.

rapid silencing of the transgene (16, 17), a pCpG-free LacZ plasmid was used. The plasmid, devoid of unmethylated 2′-deoxyribocytosine-phosphate guanosine (CpG) dinucleotides, carries an Elongation Factor–1α promoter to provide prolonged gene expression *in vivo* (18).

High concentrations of proinflammatory cytokines were previously reported in patients receiving GL67 formulations (14). Those cytokines also fluctuate in pigs under inflammatory conditions (19, 20). Therefore, IL-6 and TNF-α were measured in the BAL fluid. The concentrations detected for both cytokines were similar for the treated cohorts and the control pigs (Figures 5A and 5B), and in all the cases were within normal range. Furthermore, blood concentrations of C-reactive protein (Table E2), which normally rises in response to acute inflammation or infection, as measured in plasma samples before treatment and at the time of necroscopy (Day 4), were normal.

Cytology, performed 4 days after nebulization on the BAL of the accessory lobe of the pigs, demonstrated that the vast majority of cells were alveolar macrophages and monocytes at different stages of differentiation (Figure 5C). The percentages of lymphocytes were approximately 8.5% and 12% in both cohorts, respectively (Table 3), which is within the normal range of healthy pigs (21, 22). No statistical difference was found between the two groups of treated animals according to unpaired *t* test analysis. Very low numbers of neutrophils were detected in BAL samples from all animals, suggesting the absence of an inflammatory response.

Blood samples were collected before and after treatment, and on Day 4 before culling, and hematological and biochemical parameters were assessed for any adverse effects related to treatment. Generally, the white cell count was above normal range, both before and after treatment (Table E2), and did not demonstrate significant fluctuations after treatment. Kidney function parameters, such as creatinine, also appeared to be within normal limits. Concentrations of liver enzymes, such as alkaline phosphatase and aminotransferases (Table E2), were found to be high in most cases before and after the baseline scans and the nebulization of nanocomplexes in both treated and control animals. The elevation of serum hepatic enzyme activities has been reported after isoflurane anesthesia (23, 24), and rarely with injected ketamine (25). However, other liver function tests such as albumin and bilirubin were within reference limits.

Small abscesses were found in the neck of a control pig (B1) and in the hind leg of one of the animals from the second cohort (B2) during postmortem examination. Pig B2 exhibited a high white cell count before the study (36.4×10^9cells/L) that increased significantly after the study (43.9×10^9cells/L), as well as neutrophilia detected before and after treatment, consistent with a preexisting infection, but probably associated with the abscess rather than with the treatment. Blood results were not available for control pig B1.

DISCUSSION

Clinical studies to date suggest that the efficacy of gene therapy in adult CF patients with advanced pulmonary disease may be compromised by the impenetrable mucus layer and the inflammatory environment within the lung. Therefore, gene delivery may be more effective in children before the onset of significant lung disease. Repeated delivery to the lungs of children with CF will be necessary, because plasmid-mediated gene transfer is transient and this would be best achieved by nebulization of the vector formulation. However, to monitor the delivery process will be essential, to ensure that the vector is deposited in appropriate areas of the lung where target cells are located (i.e., those that normally express the highest concentrations of CFTR). The chloride channel is mainly expressed in the epithelial cells lining the conducting airways from the trachea to bronchioles. Aerosol properties, such as droplet size and velocity, affect distribution in the lung, and these aerosol properties may be determined and controlled by the parameter settings of the nebulizer and the type of device used. An effective imaging strategy that reflects the distribution of a nebulized vector could therefore exert a profound impact on the clinical management of patients with CF undergoing gene replacement therapy. This study sought to assess the distribution of a single dose of a nebulized gene therapy vector formulation in the porcine airways in combination with a Tc-99m radiopharmaceutical, characterizing the deposition of radiovectors by γ-camera scintigraphy.

The different regions of the lungs that showed higher radioactivity counts from the radiopharmaceutical also showed a higher number of tissue samples that were positive for the presence of the transgene, as detected by real-time PCR, with the exception of the trachea and the bronchioles. The distribution of radioactivity was compared with the localization of the transgene, as determined by real-time PCR, in tissue samples taken from different regions of the lung, to assess whether the radiocompound and the delivered gene were colocalized, and thus to assess the potential of this approach for noninvasively monitoring vector deposition in patients. Although mechanical simulators are available (26), and despite variations in the aerosol deposition because of the structure of the respiratory tract (27, 28), porcine models are used extensively for pediatric respiratory research and beyond (29–31). The porcine respiratory system was selected for these experiments because it resembles that of humans in terms of anatomy, physiology, biochemistry, and size (32, 33). Therefore, it provides a better model than small rodents for assessing the clinical potential of gene delivery vectors and their possible use for therapeutic interventions in CF. The animals were intubated, thus negating the differences in the upper airways between pigs and humans. Under these conditions, pigs are more likely to represent what happens in humans. In addition, CF pig models have been generated recently and their phenotyping and clinical features have been evaluated (33–40), which may be useful for gene correction studies of CF.

The experimental strategy involved preparing RTN vector suspensions, as previously described in studies of gene delivery to the murine lung (5, 6), and mixing them with the radiopharmaceutical Tc-99m Alb. These formulations were nebulized through an AeroEclipse II BAN nebulizer in an NGI to determine the aerodynamic characteristics of the RTN aerosol. The distribution of the radiocompound and of the plasmid DNA in

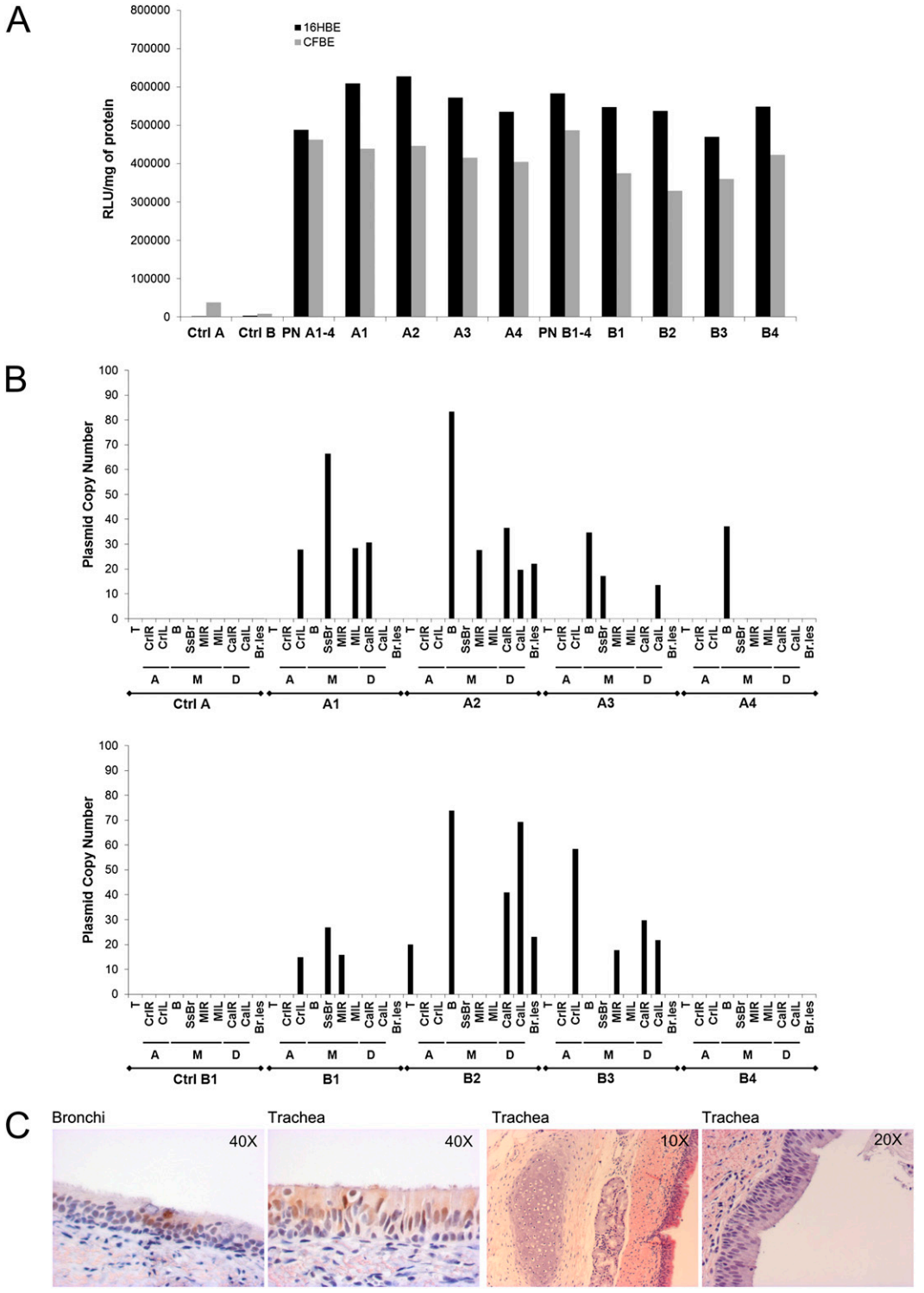

Figure 4. Transfection efficiency of the RTN formulations *in vitro* and their airway biodistribution in the porcine respiratory tree. (*A*) Small aliquots of the prenebulization suspension (PN) and of the leftover in the nebulizer chamber upon completion of nebulization from the *in vivo* experiments were used to verify their efficacy in cell culture. For control pigs, either the same water in which the complexes were formed or Tc-99m albumin nanocolloid was added to cells. After 48 hours of incubation, the normal cells (HBE14o−, *black bars*) and the CF cells (CFBE41o−, *gray bars*) were analyzed for β-galactosidase expression. PN A1–4 and PN B1–4 indicate the prenebulized suspensions given to cohort A and cohort B, respectively. All other labels on the *x* axis specify the leftover suspensions, nebulized to individual animals. (*B*) Copies of the reporter gene were detected by real-time PCR in the porcine respiratory system. The porcine tissues, collected 4 days after the nebulization of 6 ml of RTN suspension, with or without radiopharmaceuticals and containing 160 μg/ml pCpG-free LacZ plasmid DNA, were analyzed for gene expression. *Top* and *bottom*: The first and the second cohorts with their control pigs, respectively. With the exception of bronchioles, which may have been taken from more peripheral tissue, and the trachea, the different zones from where samples were excised are indicated as A, apical zones; M, middle areas; and D, diaphragmatic zones. T, trachea; CrlL and CrlR, cranial left and right lobes, respectively; MIL and MIR, middle left and right lobes, respectively; CalL and CalR, caudal left and right lobes, respectively; B, bronchi; ssB, subsegmental bronchi; Br.les, bronchioles. (*C*) Resected porcine tissues were fixed, dehydrated, wax-embedded, and probed with antibody. The two left immunostaining pictures show that the β-galactosidase encoded by the reporter gene is localized in the ciliated epithelium of the bronchi and trachea, respectively. The right tissue sections of the porcine respiratory tree, stained with hematoxylin and eosin, still indicate a normal, healthy, ciliated epithelium, after the aerosol deposition of RTNs.

each stage of the NGI was assessed. The different datasets showed that the distribution of DNA (transfection) was similar to that of Tc-99m Alb, with roughly 50% of both transfecting nanocomplexes and radiopharmaceuticals deposited between stages 4–6 of the NGI (1.36–3.30 μm), indicating an aerosol with an optimal aerodynamic size for mid–lower airway distribution.

Pigs first underwent a lung perfusion scan with MAAs to acquire a baseline scan of the lungs. After 48 hours, animals were intubated and nebulized with either the radiopharmaceutical alone, or the RTNs on their own, or the RTNs coassociated with the radiopharmaceutical (the "radiovector"). No significant changes in breathing pattern during the nebulization were observed. The

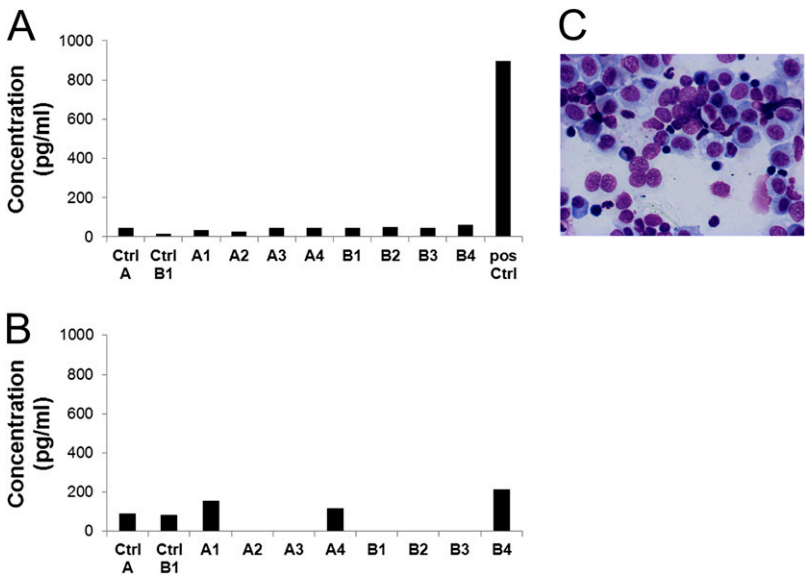

Figure 5. Analysis of inflammation markers in the bronchoalveolar lavage fluid (BALF) from the accessory lobe of a porcine lung. (*A*) The generation of an inflammatory response in pig lungs was determined by assessing the IL-6 concentrations according to ELISA. Mean values of triplicate wells are plotted. (*B*) The concentration of another key mediator of the inflammatory response and a marker of acute lung injury cytokine, such as TNF-α, was also measured in BALF by ELISA. Average values of triplicate wells are shown. (*C*) Representative cytological staining of porcine bronchoalveolar lavage indicates a normal cell composition in the specimen. pos Ctrl, positive control.

depth of breathing was sufficient, in more than 90% of breaths, to activate the AeroEclipse nebulizer to generate an aerosol in response to inspiration.

Immediately after nebulization, scintigraphy scans were acquired, showing that the radiovector was deposited predominantly in the midthoracic regions of the porcine lungs. The γ-scintigraphies were analyzed according to a relative quantification method, because the images acquired and the shape of the structures involved did not lend themselves to accurate absolute quantification. Although three-dimensional images, which better define the anatomical locations, would allow a more sensitive discrimination of the aerosol deposition (41), conventional planar methods provide reasonable qualitative results (42). In three out of four pigs (and in the control pig), the normalized central versus periphery (C/P) ratios were higher than 1, indicating that some enhancement of aerosol deposition occurred in the central airways with either radio-RTNs or Tc-99m albumin on its own. One animal showed a significant preferential deposition in the right lung, whereas another did not show central deposition. The average values for C/P ratios in the second cohort were 1.22 and 1.30 (left and right lungs, respectively), and were therefore similar to those of the control pig. Relative quantification has limitations (e.g., the tissue around the chest was considered as uniform), but the radioactivity in the bronchus may have been underestimated, in comparison with the rest of the lung, because it is located centrally, underneath the heart and the breast bone (which comprises a higher attenuating material). However, the relative quantification method minimizes this attenuation error. The midzones and diaphragmatic areas of the lungs exhibited higher radioactivity counts.

A poor correlation of imaging and molecular data from the trachea was evident, which may be associated with the process of intubation and/or the effects of the anesthetics. Although the endotracheal tube would allow efficient inhalation of the nebulized RTNs, and minimizes reflux of the radiocompound into the environment, some aerosol condenses in the tube, and on withdrawal may flow from the tube into the trachea, producing a stronger scintigraphy image. Therefore, only the distal portion of the trachea, the lining among the apical lobes of the lungs, and the area proximal to the primary bronchi were included in the quantification of radioactivity. Moreover, ketamine, although providing mild anesthesia with relatively normal breathing capability (43, 44), causes an increased production of mucus and saliva (45, 46), which may have promoted the mucociliary clearance of either the nanocomplexes or the Tc-99m RTNs from the trachea. Although atropine should counteract this effect (47), the amount used might not have been sufficient.

LacZ reporter gene delivery to the airways by either RTNs alone or by radiovectors was detected by real-time PCR in tissues of seven out of eight treated animals. The plasmid delivered was found mainly in the bronchial segments and in the midregion of the lung (the proximal main bronchi bifurcation), which correlated with the distribution of radioactivity. Despite the high radioactivity counts in the trachea, plasmid DNA was found in only one animal. Tissue sections from the bronchi and trachea (in pigs 4 and 6) showed some positive β-galactosidase immunostaining in the ciliated epithelium. Although this study was designed to focus mainly on methods of administration and the biodistribution of the RTN radiovector, rather than on optimizing transfection efficiency, we were encouraged to find significant levels of transgene expression in the conducting airway ciliated epithelium at the relatively low dose of plasmid DNA administered. The pigs were nebulized with a 6-ml suspension containing only 1 mg of pCpG-free lacZ DNA, in contrast with a recent report where gene transfer to the lungs of sheep was mediated by a liposome containing polyethylene glycol (GL67), administering 20 ml of the formulation containing 52.8 mg of human CFTR plasmid DNA (48).

The preliminary safety evaluation was encouraging, with normal BAL cytology and inflammatory profiles for TNF-α and IL-6 among all animals, and no signs of inflammation detectable by histological staining. These results suggest that the acute inflammatory response, if any, was mild and had resolved at the time of necropsy on Day 4. Hematological and biochemical analyses

TABLE 3. QUANTITATIVE EVALUATION OF BAL CYTOLOGY

Pig number	A1	A2	A3	A4	B1	B2	B3	B4	Ctrl B2
Monocytes and MØ (%)	86.8	94.0	88.0	93.3	86.6	86.2	90.2	86.2	87.9
Lymphocytes (%)	10.4	5.8	11.4	6.3	12.2	12.8	9.4	12.2	11.1
Neutrophils (%)	2.6	0.2	0.4	0.19	1.2	1.0	0.4	1.4	1.0
Eosinophils (%)	0.2		0.2	0.19				0.2	

Definition of abbreviations: BAL, bronchoalveolar lavage; Ctrl, control; MØ, macrophages.

The cell composition of the BAL from the porcine accessory lobe was assessed, and the cell populations in each specimen were expressed as percentages. The cellular composition of BAL in treated animals was comparable to that of normal pigs.

of blood samples also showed no evidence of toxicity caused by the treatment. Variations in cytology were not attributable to the treatments. There was no apparent nephrotoxicity. Although anesthesia can affect concentrations of liver enzymes, in our case, those parameters were altered before the therapeutic interventions, and albumin and bilirubin were within normal limits, suggesting that the liver function tests were normal. Further toxicological studies will be required for higher doses of RTN formulations and repeated dosing.

A subsequent study suggested that RTNs coassociated with Tc-99m diethylene-triamine-penta-acetic acid provided higher transfection efficacy than Tc-99m albumin (data not shown), and so might be better in clinical use. Further investigation in this direction will be necessary because the nebulized Tc-99m diethylene-triamine-penta-acetic acid can be released rapidly across the alveolar–capillary barrier, diffusing into the blood vessels and entering the circulation, and therefore despite its fast renal clearance (49), the interpretation of lung deposition by scintigraphy may be more difficult (50, 51).

In conclusion, we have shown that RTN radiovectors can deliver genes to the airway epithelium by nebulization, and their distribution can be monitored via a nuclear medicine approach. The radioactivity and plasmid distribution patterns suggested deposition in the conducting airways, and moreover suggested that scintigraphy is a suitable technique for monitoring nebulized gene therapy vector distribution. The data also suggest that the methodology for analyzing the tracheal distribution of radioactivity and plasmid copy numbers requires further refinement to overcome artifacts of deposition and tissue sampling. RTNs demonstrate the features of safety, distribution, and immunogenicity desirable for clinical use. Such characteristics are essential in the clinical application of CF gene therapy.

Author disclosures are available with the text of this article at www.atsjournals.org.

Acknowledgments: The authors thank the personnel of the Contract Research Unit for their technical assistance, as well as the pathologist, the Imaging Unit, and the registrars in anesthesiology at the Royal Veterinary College, without all of whom this work would not have been possible. The authors also thank Lee Davies (University of Oxford) for suggestions regarding data analysis, Ronald Edler and Martin Jackson (PerkinElmer Europe) for help in calibrating the scintillation counter, Jennifer Wootten at the Radiopharmacy of University College London Hospitals for helpful discussion regarding Tc-99m compounds, and the nurses and midwifes at the Department of Radiology, Great Ormond Street Hospital for Children, for advice on scintigraphy. The authors greatly appreciate the support of Richie Sharpe and Trudell Medical International Europe, Ltd., in providing the nebulizer AeroEclipse II BAN.

References

1. Rowe SM, Miller S, Sorscher EJ. Cystic fibrosis. *N Engl J Med* 2005;352: 1992–2001.
2. Griesenbach U, Alton EW. Gene transfer to the lung: lessons learned from more than 2 decades of CF gene therapy. *Adv Drug Deliv Rev* 2009;61:128–139.
3. Heyder J, Gebhart J, Rudolf G, Schiller CF, Stahlhofen W. Deposition of particles in the human respiratory tract in the size range 0.005–15 μm. *J Aerosol Sci* 1986;17:811–825.
4. Jaffe A, Hamutcu R, Dhawan RT, Adler B, Rosenthal M, Bush A. Routine ventilation scans in children with cystic fibrosis: diagnostic usefulness and prognostic value. *Eur J Nucl Med* 2001;28:1313–1318.
5. Manunta MD, McAnulty RJ, Tagalakis AD, Bottoms SE, Campbell F, Hailes HC, Tabor AB, Laurent GJ, O'Callaghan C, Hart SL. Nebulisation of receptor-targeted nanocomplexes for gene delivery to the airway epithelium. *PLoS ONE* 2011;6:e26768.
6. Tagalakis AD, McAnulty RJ, Devaney J, Bottoms SE, Wong JB, Elbs M, Writer MJ, Hailes HC, Tabor AB, O'Callaghan C, *et al.* A receptor-targeted nanocomplex vector system optimized for respiratory gene transfer. *Mol Ther* 2008;16:907–915.
7. Writer MJ, Marshall B, Pilkington-Miksa MA, Barker SE, Jacobsen M, Kritz A, Bell PC, Lester DH, Tabor AB, Hailes HC, *et al.* Targeted gene delivery to human airway epithelial cells with synthetic vectors incorporating novel targeting peptides selected by phage display. *J Drug Target* 2004;12:185–193.
8. Marple VA, Roberts DL, Romay FJ, Miller NC, Truman KG, Van Oort M, Olsson B, Holroyd MJ, Mitchell JP, Hochrainer D. Next generation pharmaceutical impactor (a new impactor for pharmaceutical inhaler testing): part I: design. *J Aerosol Med* 2003;16:283–299.
9. Hinds WC. Aerosol technology: properties, behavior, and measurement of airborne particles. New York: Wiley-Interscience; 1999.
10. Bennett WD, Brown JS, Zeman KL, Hu SC, Scheuch G, Sommerer K. Targeting delivery of aerosols to different lung regions. *J Aerosol Med* 2002;15:179–188.
11. Biddiscombe MF, Meah SN, Underwood SR, Usmani OS. Comparing lung regions of interest in gamma scintigraphy for assessing inhaled therapeutic aerosol deposition. *J Aerosol Med Pulm Drug Delivery* 2011;24:165–173.
12. Reinhardt AK, Bottoms SE, Laurent GJ, McAnulty RJ. Quantification of collagen and proteoglycan deposition in a murine model of airway remodelling. *Respir Res* 2005;6:30.
13. Mitchell JP, Nagel MW, Wiersema KJ, Doyle CC. Aerodynamic particle size analysis of aerosols from pressurized metered-dose inhalers: comparison of Andersen 8-stage cascade impactor, next generation pharmaceutical impactor, and Model 3321 aerodynamic particle sizer aerosol spectrometer. *AAPS PharmSciTech* 2003;4:E54.
14. Alton EW, Stern M, Farley R, Jaffe A, Chadwick SL, Phillips J, Davies J, Smith SN, Browning J, Davies MG, *et al.* Cationic lipid-mediated CFTR gene transfer to the lungs and nose of patients with cystic fibrosis: a double-blind placebo-controlled trial. *Lancet* 1999;353:947–954.
15. Ruiz FE, Clancy JP, Perricone MA, Bebok Z, Hong JS, Cheng SH, Meeker DP, Young KR, Schoumacher RA, Weatherly MR, *et al.* A clinical inflammatory syndrome attributable to aerosolized lipid–DNA administration in cystic fibrosis. *Hum Gene Ther* 2001;12:751–761.
16. Krieg AM. CpG motifs in bacterial DNA and their immune effects. *Annu Rev Immunol* 2002;20:709–760.
17. Yew NS, Zhao H, Wu IH, Song A, Tousignant JD, Przybylska M, Cheng SH. Reduced inflammatory response to plasmid DNA vectors by elimination and inhibition of immunostimulatory CpG motifs. *Mol Ther* 2000;1:255–262.
18. Gill DR, Smyth SE, Goddard CA, Pringle IA, Higgins CF, Colledge WH, Hyde SC. Increased persistence of lung gene expression using plasmids containing the ubiquitin C or elongation factor 1alpha promoter. *Gene Ther* 2001;8:1539–1546.
19. Barbe F, Atanasova K, Van Reeth K. Cytokines and acute phase proteins associated with acute swine influenza infection in pigs. *Vet J* 2011;187:48–53.
20. Sibila O, Luna CM, Agusti C, Baquero S, Gando S, Patron JR, Morato JG, Absi R, Bassi N, Torres A. Effects of glucocorticoids in ventilated piglets with severe pneumonia. *Eur Respir J* 2008;32:1037–1046.
21. Jolie R, Olson L, Backstrom L. Bronchoalveolar lavage cytology and hematology: a comparison between high and low health status pigs at three different ages. *J Vet Diagn Invest* 2000;12:438–443.
22. Gehrke I, Pabst R. Cell composition and lymphocyte subsets in the bronchoalveolar lavage of normal pigs of different ages in comparison with germfree and pneumonic pigs. *Lung* 1990;168:79–92.
23. Gunza JT, Pashayan AG. Postoperative elevation of serum transaminases following isoflurane anesthesia. *J Clin Anesth* 1992;4:336–341.
24. Ishida H, Kadota Y, Sameshima T, Nishiyama A, Oda T, Kanmura Y. Comparison between sevoflurane and isoflurane anesthesia in pig hepatic ischemia–reperfusion injury. *J Anesth* 2002;16:44–50.
25. Gonzalez Gil A, Illera JC, Silvan G, Lorenzo PL, Illera M. Changes in hepatic and renal enzyme concentrations and heart and respiratory rates in New Zealand White rabbits after anesthetic treatments. *Contemp Top Lab Anim Sci* 2002;41:30–32.
26. Steiner T, Forjan M, Kopp T, Bures Z, Drauschke A. Enhancements of a mechanical lung simulator for *ex vivo* measuring of aerosol deposition in lungs. *Biomed Techn Biomed Eng* 2012;57(Suppl. 1):799–802.
27. Kaye SR, Phillips CG, Winlove CP. Measurement of non-uniform aerosol deposition patterns in the conducting airways of the porcine lung. *J Aerosol Sci* 2000;31:849–866.
28. Phalen RF, Oldham MJ, Wolff RK. The relevance of animal models for aerosol studies. *J Aerosol Med Pulm Drug Delivery* 2008;21:113–124.

29. Dubus JC, Montharu J, Vecellio L, De Monte M, De Muret A, Goucher A, Cantagrel S, Le Pape A, Mezzi K, Majoral C, *et al.* Lung deposition of HFA beclomethasone dipropionate in an animal model of bronchopulmonary dysplasia. *Pediatr Res* 2007;61:21–25.
30. Duncan EJ, Kournikakis B, Ho J, Hill I. Pulmonary deposition of aerosolized *Bacillus atrophaeus* in a swine model due to exposure from a simulated anthrax letter incident. *Inhal Toxicol* 2009;21:141–152.
31. Sood BG, Shen Y, Latif Z, Chen X, Sharp J, Neelavalli J, Joshi A, Slovis TL, Haacke EM. Aerosol delivery in ventilated newborn pigs: an MRI evaluation. *Pediatr Res* 2008;64:159–164.
32. Rogers CS, Abraham WM, Brogden KA, Engelhardt JF, Fisher JT, McCray PB Jr, McLennan G, Meyerholz DK, Namati E, Ostedgaard LS, *et al.* The porcine lung as a potential model for cystic fibrosis. *Am J Physiol Lung Cell Mol Physiol* 2008;295:L240–L263.
33. Plog S, Mundhenk L, Bothe MK, Klymiuk N, Gruber AD. Tissue and cellular expression patterns of porcine CFTR: similarities to and differences from human CFTR. *J Histochem Cytochem* 2010;58:785–797.
34. Klymiuk N, Mundhenk L, Kraehe K, Wuensch A, Plog S, Emrich D, Langenmayer MC, Stehr M, Holzinger A, Kroner C, *et al.* Sequential targeting of CFTR by BAC vectors generates a novel pig model of cystic fibrosis. *J Mol Med (Berl)* 2012;90:597–608.
35. Ostedgaard LS, Meyerholz DK, Chen JH, Pezzulo AA, Karp PH, Rokhlina T, Ernst SE, Hanfland RA, Reznikov LR, Ludwig PS, *et al.* The DeltaF508 mutation causes CFTR misprocessing and cystic fibrosis–like disease in pigs. *Sci Transl Med* 2011;3:74ra24.
36. Meyerholz DK, Stoltz DA, Namati E, Ramachandran S, Pezzulo AA, Smith AR, Rector MV, Suter MJ, Kao S, McLennan G, *et al.* Loss of cystic fibrosis transmembrane conductance regulator function produces abnormalities in tracheal development in neonatal pigs and young children. *Am J Respir Crit Care Med* 2010;182:1251–1261.
37. Meyerholz DK, Stoltz DA, Pezzulo AA, Welsh MJ. Pathology of gastrointestinal organs in a porcine model of cystic fibrosis. *Am J Pathol* 2010;176:1377–1389.
38. Rogers CS, Hao Y, Rokhlina T, Samuel M, Stoltz DA, Li Y, Petroff E, Vermeer DW, Kabel AC, Yan Z, *et al.* Production of CFTR-null and CFTR-DeltaF508 heterozygous pigs by adeno-associated virus–mediated gene targeting and somatic cell nuclear transfer. *J Clin Invest* 2008;118:1571–1577.
39. Rogers CS, Stoltz DA, Meyerholz DK, Ostedgaard LS, Rokhlina T, Taft PJ, Rogan MP, Pezzulo AA, Karp PH, Itani OA, *et al.* Disruption of the CFTR gene produces a model of cystic fibrosis in newborn pigs. *Science* 2008;321:1837–1841.
40. Welsh MJ, Rogers CS, Stoltz DA, Meyerholz DK, Prather RS. Development of a porcine model of cystic fibrosis. *Trans Am Clin Climatol Assoc* 2009;120:149–162.
41. Fleming J, Conway J, Majoral C, Tossici-Bolt L, Katz I, Caillibotte G, Perchet D, Pichelin M, Muellinger B, Martonen T, *et al.* The use of combined single photon emission computed tomography and X-ray computed tomography to assess the fate of inhaled aerosol. *J Aerosol Med Pulm Drug Delivery* 2011;24:49–60.
42. Phipps PR, Gonda I, Bailey DL, Borham P, Bautovich G, Anderson SD. Comparisons of planar and tomographic gamma scintigraphy to measure the penetration index of inhaled aerosols. *Am Rev Respir Dis* 1989;139:1516–1523.
43. Kostopanagiotou G, Kalimeris K, Christodoulaki K, Nastos C, Papoutsidakis N, Dima C, Chrelias C, Pandazi A, Mourouzis I, Pantos C. The differential impact of volatile and intravenous anaesthetics on stress response in the swine. *Hormones (Athens)* 2010;9:67–75.
44. Linkenhoker JR, Burkholder TH, Linton CG, Walden A, Abusakran-Monday KA, Rosero AP, Foltz CJ. Effective and safe anesthesia for Yorkshire and Yucatan swine with and without cardiovascular injury and intervention. *J Am Assoc Lab Anim Sci* 2010;49:344–351.
45. Bergman SA. Ketamine: review of its pharmacology and its use in pediatric anesthesia. *Anesth Prog* 1999;46:10–20.
46. Chum H, Pacharinsak C. Endotracheal intubation in swine. *Lab Anim (NY)* 2012;41:309–311.
47. Kye YC, Rhee JE, Kim K, Kim T, Jo YH, Jeong JH, Lee JH. Clinical effects of adjunctive atropine during ketamine sedation in pediatric emergency patients. *Am J Emerg Med* 2012;30:1981–1985.
48. McLachlan G, Davidson H, Holder E, Davies LA, Pringle IA, Sumner-Jones SG, Baker A, Tennant P, Gordon C, Vrettou C, *et al.* Preclinical evaluation of three non-viral gene transfer agents for cystic fibrosis after aerosol delivery to the ovine lung. *Gene Ther* 2011;18:996–1005.
49. Ciofetta G, Piepsz A, Roca I, Fisher S, Hahn K, Sixt R, Biassoni L, De Palma D, Zucchetta P. Guidelines for lung scintigraphy in children. *Eur J Nucl Med Mol Imaging* 2007;34:1518–1526.
50. Coates AL, Green M, Leung K, Louca E, Tservistas M, Chan J, Ribeiro N, Charron M. The challenges of quantitative measurement of lung deposition using 99mTc-DTPA from delivery systems with very different delivery times. *J Aerosol Med* 2007;20:320–330.
51. Coates G, O'Brodovich H. Measurement of pulmonary epithelial permeability with 99mTc-DTPA aerosol. *Semin Nucl Med* 1986;16:275–284.
52. Marple VA, Olson BA, Santhanakrishnan K, Roberts DL, Mitchell JP, Hudson-Curtis BL. Next generation pharmaceutical impactor: a new impactor for pharmaceutical inhaler testing: part III: extension of archival calibration to 15 L/min. *J Aerosol Med* 2004;17:335–343.